Chemical Engineering Journal 247 (2014) 33–41

Contents lists available at ScienceDirect

Chemical Engineering Journal

journal homepage: www.elsevier.com/locate/cej

Strain sensing behavior and dynamic mechanical properties of carbon nanotubes/nanoclay reinforced wood polymer nanocomposite

Ankita Hazarika, Tarun K. Maji *

Department of Chemical Sciences, Tezpur University, Assam 784028, India

HIGHLIGHTS

- Wood polymer nanocomposites (WPNC) were prepared by impregnation method.
- Modification of MWCNT was studied by Raman spectroscopy.
- Efficient load transfer was found from MWCNT to wood/polymer.
- WPNC exhibited an improvement in dynamic mechanical properties.
- Activation energy for the relaxation process increased for the composites.

GRAPHICAL ABSTRACT

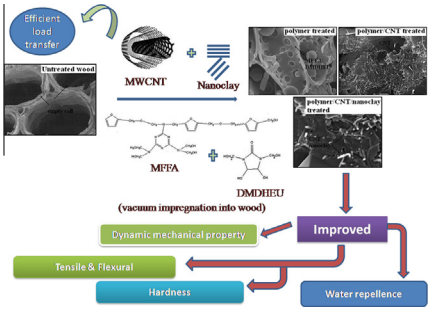

ARTICLE INFO

Article history:
Received 30 September 2013
Received in revised form 21 January 2014
Accepted 21 February 2014
Available online 12 March 2014

Keywords:
Wood
Nanocomposites
Multiwalled carbon nanotubes
Raman spectroscopy
Mechanical properties

ABSTRACT

Wood polymer nanocomposites (WPNC) was prepared consisting of multiwalled carbon nanotubes (MWCNT) and nanoclay by vacuum impregnation of melamine formaldehyde furfuryl alcohol copolymer and 1,3-dimethylol 4,5-dihydroxy ethylene urea, a crosslinking agent. X-ray diffraction study indicated a decrease in crystallinity of wood cellulose in the composites. Strain dependent Raman spectroscopy showed efficient load transfer from the wood/polymer to the nanotubes indicating better interfacial interaction. The surface morphology of the composites was studied by scanning electron microscope. Dynamic mechanical analysis showed an enhancement in elastic modulus, loss modulus and damping index for the WPNC. At a fixed nanoclay loading, with the increase in the content of MWCNT in the composites, the apparent activation energy for the relaxation process in the glass transition region increased. Tensile, flexural, hardness and water repellence properties improved significantly after incorporation of MWCNT into the composites.

1. Introduction

Wood polymer composites (WPC) have gained significant popularity in the recent years as it can be a replacement for solid wood due to its advantageous properties for different construction purposes and outdoor applications. The service life of wood can be enhanced through chemical modification by the use of suitable chemicals [1]. Fig wood (*Ficus hispida*), a type of softwood, is not appropriate for structural applications due to its poor dimensional, mechanical and other physical properties. This wood can be made value added by forming composites with polymers. WPC prepared by vacuum impregnation of polymers are suitable for various applications like outdoor deck floors, railings, fences, cladding and siding, park benches, window and door frames and indoor furnitures [2,3]. The application of vacuum during the process of impregnation evacuates air from the pores of the wood samples and helps in penetration of monomers and nanofillers into its empty spaces. However, the simultaneous use of the combination of vacuum and pressure leads to better penetration of polymer/

* Corresponding author. Tel.: +91 03712 267007x5053; fax: +91 03712 267005.
E-mail address: tkm@tezu.ernet.in (T.K. Maji).

http://dx.doi.org/10.1016/j.cej.2014.02.069
1385-8947/

nanofillers into the wood so as to attain further improvement in properties. The properties of WPC can be improved further by the use of nano materials.

The application of nano materials such as nanoclay and carbon nanotubes (CNT) to reinforce polymer composites has drawn the attention with the advancement of nanotechnology. Nanoclay treated WPC as in situ reinforcement has been reported to improve its properties significantly [4]. CNTs are considered to be new emergent multifunctional materials that have outstanding mechanical and thermal properties which make it a potential contender for a wide variety of applications [5]. Poor interfacial interaction between polymer and CNT as well as sturdy intermolecular Van der Waals interactions among the nanotubes render formation of its aggregates [6]. Therefore it is essential to modify the surface of CNT with some functional groups [7]. Apart from improvement in mechanical properties, incorporation of CNT in combination with nanoclay in poly(methylmethacrylate) has been reported to enhance thermal stability and flame retardancy of the composites [8]. Few reports are available pertaining to the combined use of CNT and nanoclay in WPC. Hence there is lot of scope to do further work in this area.

The use of water as a solvent has drawn special attention for a sustainable environment instead of using petroleum based diluents. Furfurylated wood results in significant improvement in dimensional stability and durability but the treated wood does not show improvement in the bending strength and the modulus of elasticity (MOE) [9]. Melamine formaldehyde resin is capable of forming hydrogen bonds leading to an improvement in dimensional, mechanical and thermal properties of the composite [10]. Therefore a copolymer of melamine formaldehyde and furfuryl alcohol (MFFA) can lead to an overall improvement in properties of the composites.

Dynamic mechanical analysis (DMA) is an effective tool to study the viscoelastic behavior of the materials under various conditions of stress, temperature for diverse applications. The dynamic parameters such as storage modulus E', loss modulus E'' and mechanical damping $\tan\delta$ of nanocomposite provide an important insight to study the interaction between wood, polymer and the nanoparticles [4].

The vibrational modes and the structure of CNTs have been widely studied by the Raman spectroscopic technique [11]. The characteristic features of Raman spectroscopy of multiwalled carbon nanotubes (MWCNT) are appearance of peak at about 1345 and 1572 cm^{-1} which can be assigned to the D-band and the G-band of MWCNT respectively [12]. D-band is associated with the scattering of an electron by phonon emission by the disordered sp^3 hybridized carbon network and the local defects that initiate from structural imperfections. G-band is related to the ordered sp^2 hybridized carbon network that is associated with the tangential C–C stretching vibration [13]. A local strain will induce in CNT as mechanical load is transmitted from polymer matrix to CNT. The C–C bond vibration that occurs due to the local strain can be analyzed by Raman spectroscopy [14].

Keeping the above in view, the present work has been aimed to prepare MFFA prepolymer and 1,3-dimethylol 4,5-dihydroxyethylene urea (DMDHEU) for impregnation into wood in presence of MWCNT and nanoclay. The main objective is to study the synergistic effect of MWCNT and nanoclay on Raman peak shift due to the strain sensing behavior of the composites under loading, DMA, tensile, flexural and water repellent properties of the prepared composites.

2. Methods

2.1. Materials

Fig wood (*F. hispida*) was collected locally. Melamine, furfuryl alcohol, glyoxal, maleic anhydride and formaldehyde were purchased from Merck (Mumbai, India). Nanomer (clay modified by 15–35 wt% octadecylamine and 0.5–5 wt% aminopropyltriethoxy silane, Aldrich, USA), and MWCNT CM-250 (5–10 nm inner diameter, 60–100 nm outer diameter, 250 μm length, Sigma Aldrich, Korea) were used as received. All other chemicals used were of analytical grade.

2.2. Modification of MWCNT

A mixture of potassium hydroxide and ethanol was prepared and 5 g of MWCNT was added to it. The reaction mixture was placed in an ultrasonic bath for 24 h at 80 °C. The resulting mixture was filtered and repeatedly washed with deionized water until the pH value reached 7. Finally it was dried overnight in vacuum oven at 45 °C. The product obtained was the MWCNT-OH.

2.3. Preparation of the MFFA copolymer

Melamine (31.53 g) and formaldehyde (60.81 ml) were taken in molar ratio of 1:3 and polymerized by bulk polymerization at 80–85 °C by maintaining pH at 8.5–9.0 with Na_2CO_3. 1 mole of furfuryl alcohol (43.40 ml) was added to the aqueous solution of methylol melamine followed by addition of maleic anhydride as catalyst and finally polymerized for another 45 min. The viscosity (at 30 °C) of different batches of MFFA copolymer thus prepared was almost similar as judged by Ubbelohde viscometer.

2.4. Preparation of DMDHEU crosslinker

The molar ratio of n(glyoxal), n(urea), n(formaldehyde) were taken as 1:1.10:1.95 for synthesis of DMDHEU. Urea (6.6 g) was added slowly to an aqueous solution of glyoxal (4.5 ml) under nitrogen purge .The pH of the reaction mixture was adjusted to a approximately 5.5. The reaction mixture was then heated to 50 °C and allowed to stir for 24 h. The reaction was cooled to room temperature, neutralized and evaporated to near dryness by rotary evaporator to yield crude 4,5-dihydroxyethylene urea (DHEU). DHEU was added to an aqueous formaldehyde (15.8 ml) solution and pH was adjusted to 8.2–8.5. The reaction mixture was heated to approximately 50 °C and allowed to stir for 24 h. The reaction mixture was then allowed to cool to room temperature, neutralised and kept for subsequent use [15].

2.5. Dispersion of MWCNT and nanoclay in MFFA copolymer

MWCNT and nanoclay were swelled in FA-water mixture for 24 h with mechanical stirring. FA-water mixture can swell the mixture of MWCNT as well as nanoclay and is a good solvent for the MFFA copolymer. The dispersed MWCNT and nanoclay was then sonicated for 30 min. Now MFFA was slowly added to the dispersed MWCNT and nanoclay under stirring condition. This mixture was further sonicated for 15 min and kept ready for use.

2.6. Preparation of wood polymer composites (WPC)

All the samples were cut into dimensions following ASTM (American Society for Testing and Materials) measurements and oven dried at 105 °C to constant weight and was then taken in an impregnation chamber. The samples were cut into 2.5 cm × 1 cm × 2.5 cm for water uptake test and hardness test. The wood samples for tensile and flexural test were cut into 10 cm × 0.5 cm × 2 cm and 1 cm × 1 cm × 16 cm respectively. The samples were cut into 5 cm × 1.25 cm × 0.35 cm for the dynamic mechanical analysis (DMA) test. Vacuum was applied for a specific time period for removing the air from the pores of the wood samples before addition of the respective prepolymeric

mixture. The samples were kept immersed in the impregnation chamber containing prepolymeric mixture for 6 h after attaining atmospheric pressure. The samples were then taken out, wiped, wrapped in aluminium foil and cured at 90 °C for 24 h in an oven. The cured samples were then Soxhlet extracted to remove homopolymers, if any, formed during impregnation. The solvent used in the process of extraction was a mixture of acetone and ethanol (1:1 molar ratio).

The optimized conditions for getting maximum improvement in properties were 500 mm Hg vacuum, 6 h time of impregnation, 5:1 (MFFA:FA-water) prepolymer concentration, 1% (w/w) maleic anhydride, 3 ml DMDHEU, 3 phr nanoclay, and 0.5–1.5 phr modified MWCNT. The polymer taken was 100 ml and solvent taken was 20 ml keeping the ratio of polymer (MFFA) and solvent (FA-water) in 5:1. In all the samples treated with nanoparticles, MWCNT was varied from 0.5 to 1.5 phr keeping the amount of nanoclay fixed at 3 phr. Five samples of each treatment were used to study the properties and the average value were taken.

3. Measurements

NMR (Nuclear Magnetic Resonance) spectra of MFFA and DMDHEU were recorded with 400 MHz FTNMR (JEOL, Japan) spectrometer by using DMSO (dimethyl sulphoxide) as solvent and TMS (trimethyl silane) as internal standard.

Weight percent gain (WPG) after polymer loading was calculated according to the formula

$$\text{WPG} = (W_2 - W_1)/W_1 \times 100$$

where 'W_1' was oven dry weight of wood blocks before polymer treatment and 'W_2' was oven dry weight of blocks after polymer treatment.

Percentage volume increase after impregnation of wood samples was calculated by the formula:

$$\%\ \text{Volume increase} = (V_2 - V_1)/V_1 \times 100$$

where 'V_1' was oven dry volume of the untreated wood and 'V_2' was oven dry volume of the treated wood.

The hardness of the samples was measured by using a durometer (model RR12) according to ASTM D2240 method and expressed as shore D hardness.

The crystallographic studies were done by X-ray diffraction (XRD) analysis using Rigaku X-ray diffractometer (Miniflax, UK) and employing Cu Kα radiation (λ = 0.154 nm), at a scanning rate of 2° min^{-1} with an angle ranging from 2° to 60°.

Raman spectra was collected in the back scattering geometry using a Micro-Raman Microscope made by WITec (USA) using 532 nm excitation laser with polarizer and the analyzer parallel to each other. For the deformation of the composites loaded with MWCNT, the samples were strained under Raman spectrometer by inserting into a four-point bending rig. The strains applied to the samples were increased step wise at intervals of about 0.1% until failure. Three Raman spectra were collected for each strain level from random areas of the samples and the presented results were the average of these three spectra. Since the position of G′-band was observed at 2600 cm^{-1}, the spectra were centered at that region.

The microstructure of the fracture surfaces of untreated and treated wood samples were studied and analyzed by using a scanning electron microscope (SEM Nanonova 230), manufactured by FEI (Field Emission Inc.) (Hillsboro, OR, USA).

DMA was performed using TA instruments Q800 according to ASTM D-7031. Specimens were scanned over a temperature range of 25–200 °C. Frequency of the oscillation was performed at 1, 3, 5 and 10 Hz ramped at 2 °C/min to 200 °C. Storage modulus, loss modulus and mechanical loss factor ($\tan\delta$) were recorded and plotted against temperature.

The tensile and flexural tests for untreated wood and WPCs were carried out using Universal Testing Machine (Zwick, model Z010) at a crosshead speed of 2 mm/min at room temperature according to ASTM D-638 and D-790 respectively.

Both untreated and treated wood samples were immersed in distilled water at room temperature (30 °C) and weights were taken after 0.5, 2, 6, 24, 48, 96, 120, 144, and 168 h. It is expressed as

$$\text{Water uptake}\ (\%) = (W_t - W_d)/W_d \times 100$$

where W_d is the oven dry weight; and W_t is the weight after immersion in distilled water for a specified time period.

Datas for WPG, volume increase%, hardness, tensile and flexural were expressed as mean of standard deviation (±SD). Results were statistically analyzed using one way ANOVA followed by Tukey HSD test. Five samples of each category were tested.

4. Results and discussion

4.1. NMR study of MFFA and DMDHEU

The carbon-13 nuclear magnetic resonance (^{13}C NMR) spectra of MFFA and DMDHEU are shown in Fig. 1. MFFA copolymer (Fig. 1a) showed a peak at 49.3 ppm for linear methylene unit (–N–CH_2–Fu–) and another singlet appeared at 56.06 ppm due to the presence of (Fu–CH_2OH). Peaks appearing at 60.24 and 64.53 ppm were attributed to –N–CH_2OH and –O–CH_2–Fu respectively. The appearance of signals at 68.67–89.97 ppm was assigned to the methylene ether linkage (N–CH_2–O–CH_2–N). The peak at 107.42 ppm was due to the 3-position of terminal furan ring. The signals appearing at 109.63 and 110 ppm were due to the presence of 3-position of terminal furan ring which has the substituted –OH

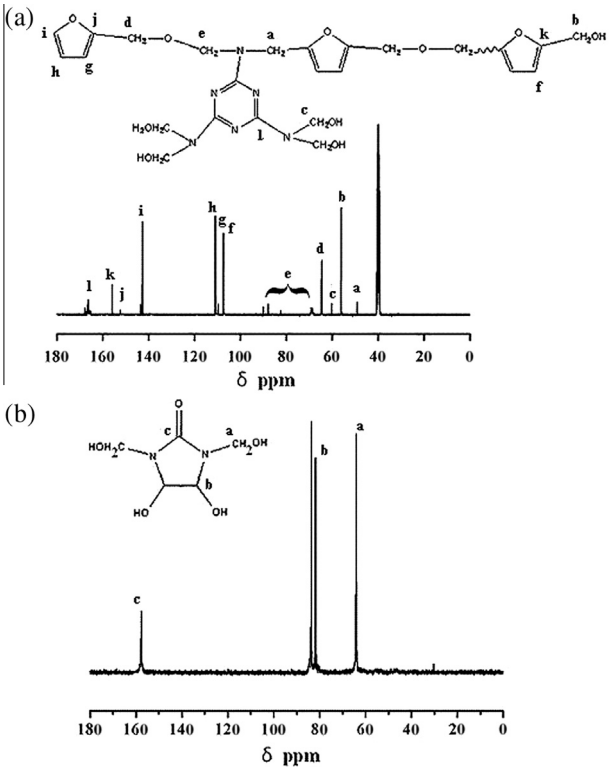

Fig. 1. NMR spectra of (a) MFFA and (b) DMDHEU.

group and 4 position of terminal furan rings. 5-position of terminal furan ring was characterized by the presence of signals at 142.57–143.43 ppm. The signals at 152.25 and 155.83 ppm were assigned to 2-position of terminal furan ring which has the substituted –OH group and 2-position of terminal furan ring which has the unsubstituted –OH group respectively. Other peaks at 166.45 and 167.66 ppm were attributed to triazine carbon of methylol melamine and unsubstituted triazine nucleus [16]. The NMR spectrum of DMDHEU (Fig. 1b) showed signals at 159.84, 81.81 and 64.01 ppm due to the presence of carbonyl carbon, –CHOH and –$NHCH_2OH$ respectively [17].

4.2. Effect of variation of MWCNT on polymer loading (WPG%), volume increase and hardness

It was observed from Table 1 that polymer loading (WPG), volume increase, and hardness were found to increase for the samples treated with MFFA/DMDHEU. The deposition of polymer into the void spaces of wood was enhanced by DMDHEU due to its interaction with wood and polymer through its hydroxyl groups [18]. Addition of MWCNT to MFFA/DMDHEU did not significantly influence its WPG and the volume increase, but a remarkable enhancement in hardness was observed. When nanoclay was added to the composites treated with MFFA/DMDHEU/MWCNT, an overall improvement in properties was observed. At fixed nanoclay loading (3 phr), a slight increase in WPG and volume increase (%) were observed with the increase in the amount of MWCNT. The hardness value was found to increase appreciably. A significant increase in hardness value was reported by Uddin et al. after incorporation of MWCNT into copper matrix composite [19]. The increased hardness value was due to interfacial interaction of surface hydroxyl groups of MWCNT with the hydroxyl groups of wood, MFFA, DMDHEU and nanoclay.

4.3. XRD study

The XRD pattern of MWCNT-OH, nanoclay, untreated wood and WPC is shown in Fig. 2. A sharp diffraction peak for MWCNT-OH appeared at 25.85° (002 crystal plane graphite). Appearance of peaks of medium intensity at 42.87° and 44.82° could be attributed to the 002, 100 and 101 reflections of graphite (curve a) [20]. The organically modified nanoclay (curve b) showed a sharp peak at $2\theta = 4.3°$. The gallery distance calculated by using Bragg's equation was found to be 2.05 nm. Other peaks appeared at 21.01° and 35.54° due to the presence of alkyl chain of the surfactant [21]. As cellulose is the chief constituent of wood, it showed a wide diffraction peak at $2\theta = 22.88°$ due to the 002 crystal plane of cellulose. The other crystal plane of cellulose i.e. 101 plane showed small peak at 15.02° (curve c) [22]. WPC treated with MWCNT showed a decrease in the intensity of the crystallinity peak of cellulose at 22.88°. The peak at 15.02° corresponding to 101 plane of cellulose became dull. The characteristic peaks of MWCNT at $2\theta = 42.87°$ and 44.82° appeared in the diffractograms of the composites (curve d). Curve (e–g) represents the X-ray diffraction pattern of WPC treated with 3 phr nanoclay and different percentages of MWCNT (0.5–1.5 phr). The disappearance of the first

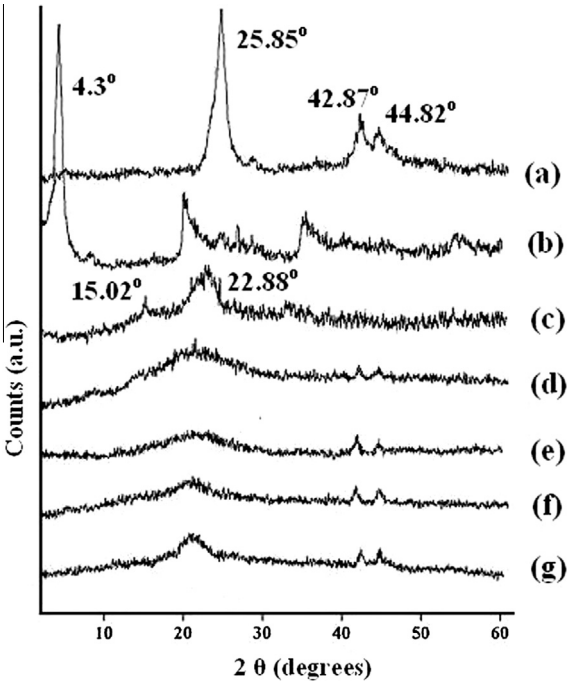

Fig. 2. X-ray diffraction of (a) modified MWCNT, (b) nanoclay, (c) untreated wood and wood treated with, (d) MFFA/DMDHEU/MWCNT (1.5 phr), (e) MFFA/DMDHEU/nanoclay/MWCNT (0.5 phr), (f) MFFA/DMDHEU/MWCNT (1.0 phr) and (g) MFFA/DMDHEU/nanoclay/MWCNT (1.5 phr).

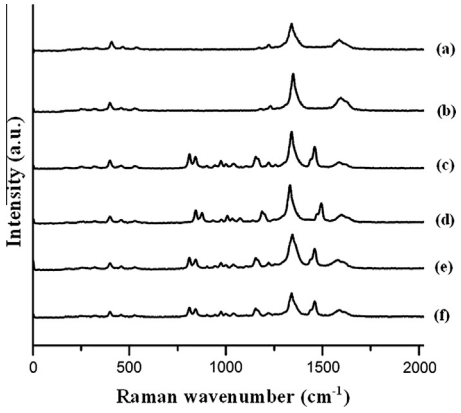

Fig. 3. Raman spectra of (a) unmodified MWCNT, (b) MWCNT-OH and wood treated with, (c) MFFA/DMDHEU/nanoclay/MWCNT (0.5 phr), (d) MFFA/DMDHEU/nanoclay/MWCNT (1.0 phr), (e) MFFA/DMDHEU/MWCNT (1.5 phr) and (f) MFFA/DMDHEU/nanoclay/MWCNT (1.5 phr).

Table 1
Effect of variation of MWCNT on weight% gain (WPG), volume increase, hardness and activation energy.

Samples particulars	Weight gain (%) (WPG)	Volume increase (%)	Hardness (Shore D)	Activation energy (E_a kJ/mol)
Untreated	–	–	47.0 (±0.8)	118.8
Samples treated with MFFA/FA-water/DMDHEU/nanoclay/MWCNT				
100/20/3/0/0	28.3 (±0.2)	2.0 (±0.1)	61.1 (±0.4)	129.4
100/20/3/3/0	35.0 (±0.3)	2.7 (±0.4)	72.4 (±0.2)	–
100/20/3/0/1.5	31.1 (±0.4)	2.6 (±0.5)	92.5 (±0.3)	273.5
100/20/3/3/0.5	35.6 (±0.2)	2.7 (±0.7)	88.3 (±0.7)	243.3
100/20/3/3/1.0	36.5 (±0.2)	2.8 (±0.6)	91.0 (±0.8)	260.4
100/20/3/3/1.5	37.5 (±0.5)	2.9 (±0.4)	95.6 (±0.3)	282.3

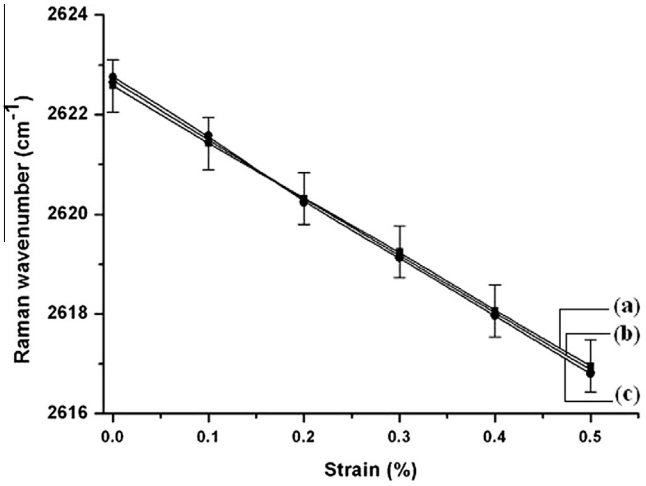

Fig. 4. G′-band shift as a function of strain (%) for wood treated with, (a) MFFA/DMDHEU/nanoclay/MWCNT (0.5 phr), (b) MFFA/DMDHEU/nanoclay/MWCNT (1.0 phr) and (c) MFFA/DMDHEU/nanoclay/MWCNT (1.5 phr).

diffraction peak for the nanoclay in the composites indicated that either the nanoclay layers became delaminated or layers of nanoclay were separated so that it was not possible to detect by XRD. The intensity of the peak appearing at 22.88° of wood cellulose was found to decrease with the increase in the amount of MWCNT and the small peak at 15.02° became dull. The nanoparticles were inserted into the amorphous region of wood cellulose suggesting a decrease in the crystallinity of wood cellulose due to incorporation of nanoparticles into the composites [15,22–24]. However, the characteristic peak of MWCNT at 42.87° and 44.82° was found in the diffractograms of the WPC and the intensity became more pronounced as the amount of MWCNT was increased.

4.4. Raman study

The functionalization of the MWCNT was investigated by use of Raman spectroscopy. The hydroxyl functionalized MWCNT (Fig. 3) showed an enhanced area ratio of D-band to G-band compared to the pristine MWCNT which could be attributed to the microstructural changes in the tubes (Fig. 3). The ratio between the intensity of D-band (I_D) and G-band (I_G) peaks is used to indicate the degree of crystallinity and is typically taken as a standard measurement of the surface defects of CNTs [25], purity of the CNTs [26] and hence the structural modification of the sidewall. An increase in the intensity ratio of the bands I_D–I_G due to MWCNT surface functionalization was reported in the literature [27]. The surface modification of MWCNT was reported by the visible increase of the I_D/I_G ratio. The D-band indicates the multi crystal or amorphous carbon-based materials, whereas the G-band indicated the graphite crystal structure in the carbon-based materials. Further, it was observed from the spectra of WPC loaded with MWCNT that the I_D/I_G ratio increased with the increase in the amount of MWCNT. This was due to interaction of polymer and wood with hydroxyl group of MWCNT.

A change in both interatomic distance and vibrational frequencies of some of the normal modes of a material caused the shifting of Raman peak under an applied strain [28]. When strain was applied, the C–C bond vibration of MWCNT was changed due to transfer of load from wood/polymer to MWCNT. With the increase in the amount of strain, a significant shift of the G′-band of MWCNT was observed (Fig. 4). The defect functionalized MWCNT enhanced the interfacial interaction between MWCNT, polymer and wood through its hydroxyl groups. It was observed from Fig. 4 that there was a linear relationship (with a negative slope) between the G′-band shift and the applied strain for the WPC samples loaded with MWCNT. The higher the applied strain, the higher was the G′-band shift indicating a good interfacial interaction between the MWCNT and the MFFA/wood. At a fixed loading of nanoclay, WPC treated with 0.5, 1 and 1.5 phr MWCNT showed slopes of 11.2, 12.1 and 13.3 cm^{-1}/strain%, respectively calculated from the G′-band shift rates. Wood treated with MFFA/DMDHEU/MWCNT (1.5 phr) showed shifting of G′-band similar to those of samples treated with MFFA/DMDHEU/nanoclay/MWCNT (1.5 phr) (not shown). The effectiveness of load transfer in the composites was determined by the slope of the G′-band shift versus the strain curve. From

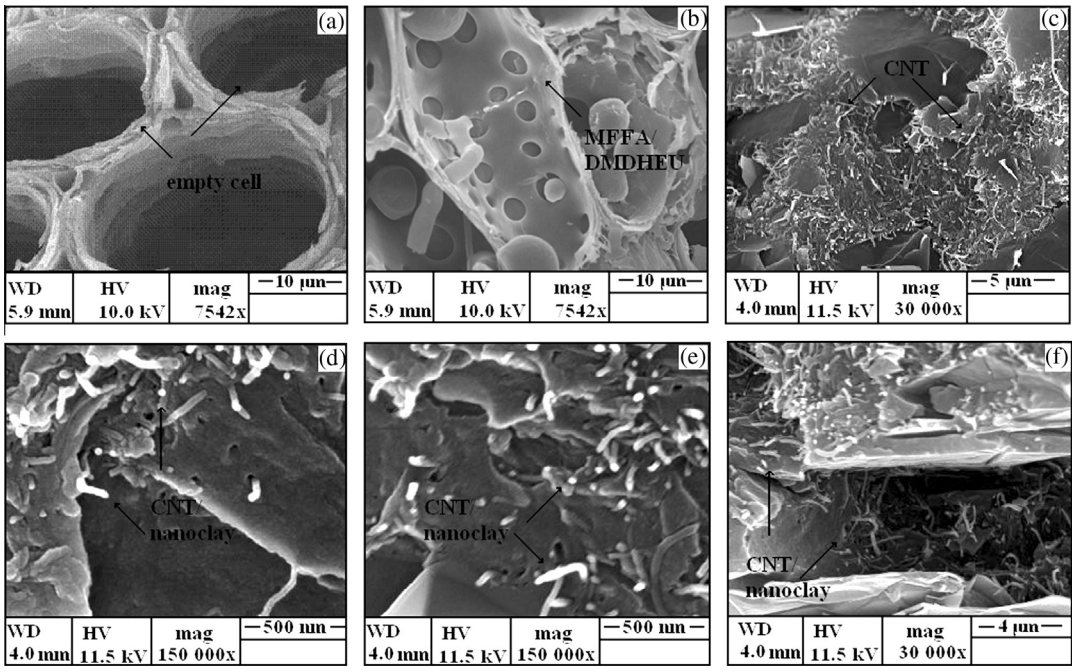

Fig. 5. Scanning electron micrograph of (a) untreated wood and wood treated with, (b) MFFA/DMDHEU, (c) MFFA/DMDHEU/nanoclay/MWCNT (0.5 phr), (d) MFFA/DMDHEU/nanoclay/MWCNT (1.0 phr), (e) MFFA/DMDHEU/MWCNT (1.5 phr) and (f) MFFA/DMDHEU/nanoclay/MWCNT (1.5 phr).

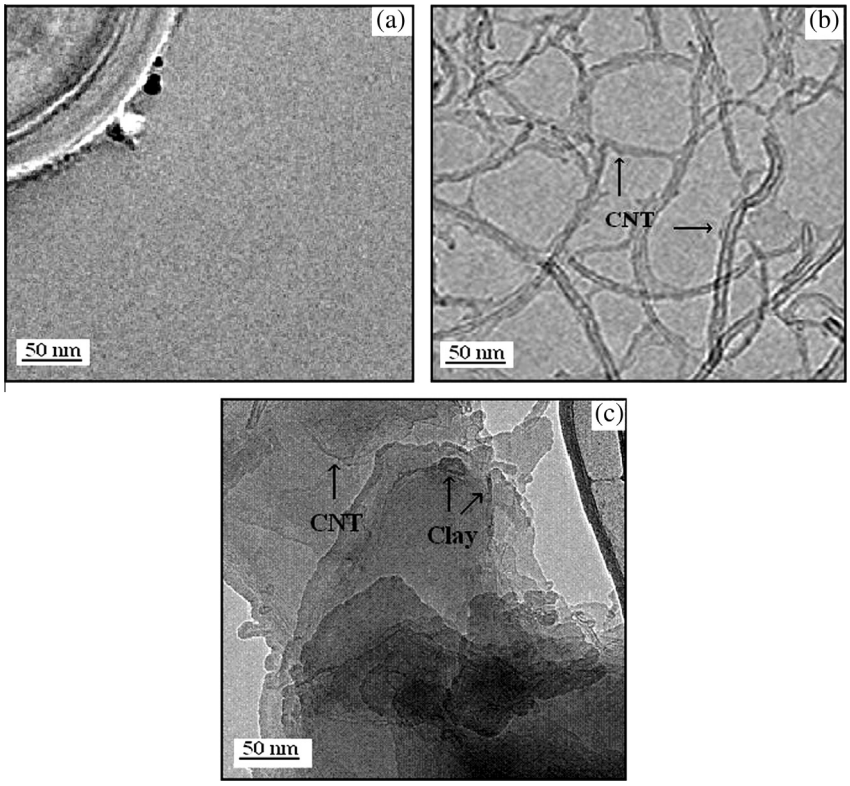

Fig. 6. Transmission electron micrographs of (a) untreated wood and wood treated with, (b) MFFA/DMDHEU/MWCNT (1.5 phr) and (c) MFFA/DMDHEU/MWCNT (1.5 phr)/nanoclay.

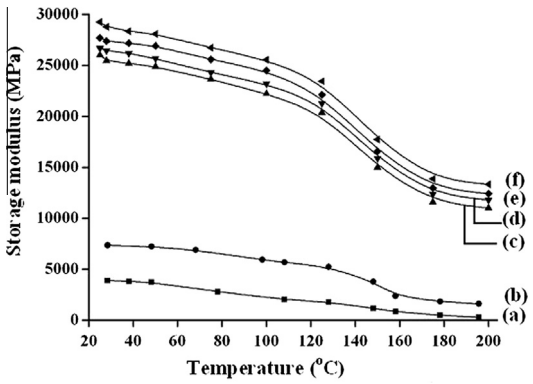

Fig. 7A. Storage modulus of (a) untreated wood and wood treated with, (b) MFFA/DMDHEU, (c) MFFA/DMDHEU/nanoclay/MWCNT (0.5 phr), (d) MFFA/DMDHEU/nanoclay/MWCNT (1.0 phr), (e) MFFA/DMDHEU/MWCNT (1.5 phr) and (f) MFFA/DMDHEU/nanoclay/MWCNT (1.5 phr).

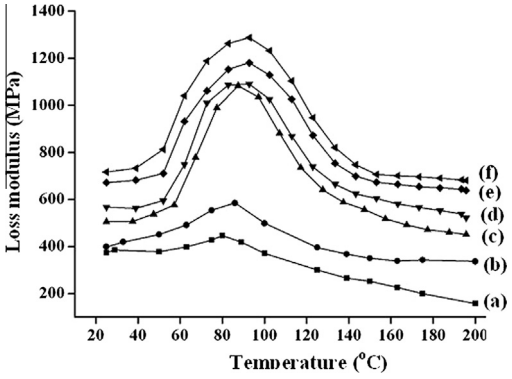

Fig. 7B. Loss modulus of wood treated with (a) untreated wood and wood treated with, (b) MFFA/DMDHEU, (c) MFFA/DMDHEU/nanoclay/MWCNT (0.5 phr), (d) MFFA/DMDHEU/nanoclay/MWCNT (1.0 phr), (e) MFFA/DMDHEU/MWCNT (1.5 phr) and (f) MFFA/DMDHEU/nanoclay/MWCNT (1.5 phr).

Fig. 3, it was further observed that the slope became steeper with the increase in the content of MWCNT in the composites. Load transfer occurred more effectively to the composites having a steeper slope [29]. The higher the amount of MWCNT, the more efficient was the load transfer from wood/polymer to MWCNT. The increase in slope (20%) with the increase in MWCNT content indicated better stress transfer at the interface by the distributed MWCNT in the composites.

4.5. Morphological studies of the WPNC

4.5.1. Scanning electron microscopy

The scanning electron micrographs of untreated and treated wood samples are shown in Fig. 5. Untreated wood samples have empty pits and parenchymas (Fig. 5a) which were filled up by the MFFA/DMDHEU due to treatment with polymer (Fig. 5b). In the micrograph of samples treated with MFFA/DMDHEU/MWCNT, a homogenous dispersion of MWCNT was observed (Fig. 5c). Addition of nanoclay and MWCNT could be seen as some white spots and cylindrical structures (Fig. 5d–f).

4.5.2. Transmission electron microscopy

TEM micrographs of untreated and treated wood samples are shown in Fig. 6. No orientation of cell wall components were observed in untreated wood (Fig. 6a). The dispersion of MWCNT and nanoclay was observed as some cylindrical and dark slices in the micrograph. It was observed that the MWCNT was dispersed uniformly in the wood samples treated with MFFA/DMDHEU/

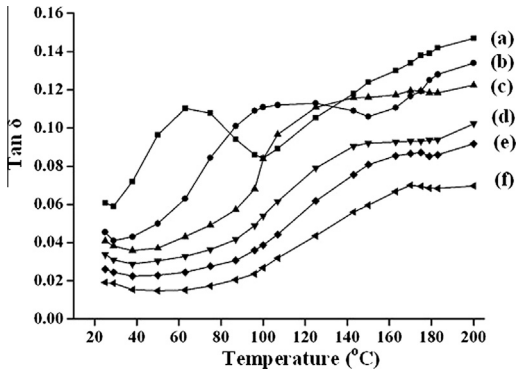

Fig. 7C. Tan δ of (a) untreated wood and wood treated with, (b) MFFA/DMDHEU, (c) MFFA/DMDHEU/nanoclay/MWCNT (0.5 phr), (d) MFFA/DMDHEU/nanoclay/MWCNT (1.0 phr), (e) MFFA/DMDHEU/MWCNT (1.5 phr) and (f) MFFA/DMDHEU/nanoclay/MWCNT (1.5 phr).

MWCNT as revealed by the TEM study (Fig. 6b). The dispersion of nanoclay along with MWCNT was also found to be distributed homogenously in the micrograph of the samples treated with MFFA/DMDHEU/MWCNT/nanoclay (Fig. 6c). In order to improve certain properties of WPC, addition of clay to MWCNT is very relevant.

4.6. Dynamic mechanical analysis

4.6.1. Storage modulus

The storage moduli of untreated and treated wood samples are represented in Fig. 7A. The storage modulus decreased steeply near the glass transition temperature (T_g) of wood (50–120 °C) due to the viscoelastic behavior of wood. In all the cases, the storage modulus was found to decrease with the increase in temperature because of increased chain mobility of the wood cell wall polymeric components. MFFA copolymer and DMDHEU interacted with hydroxyl groups of wood cell wall forming a networked structure.

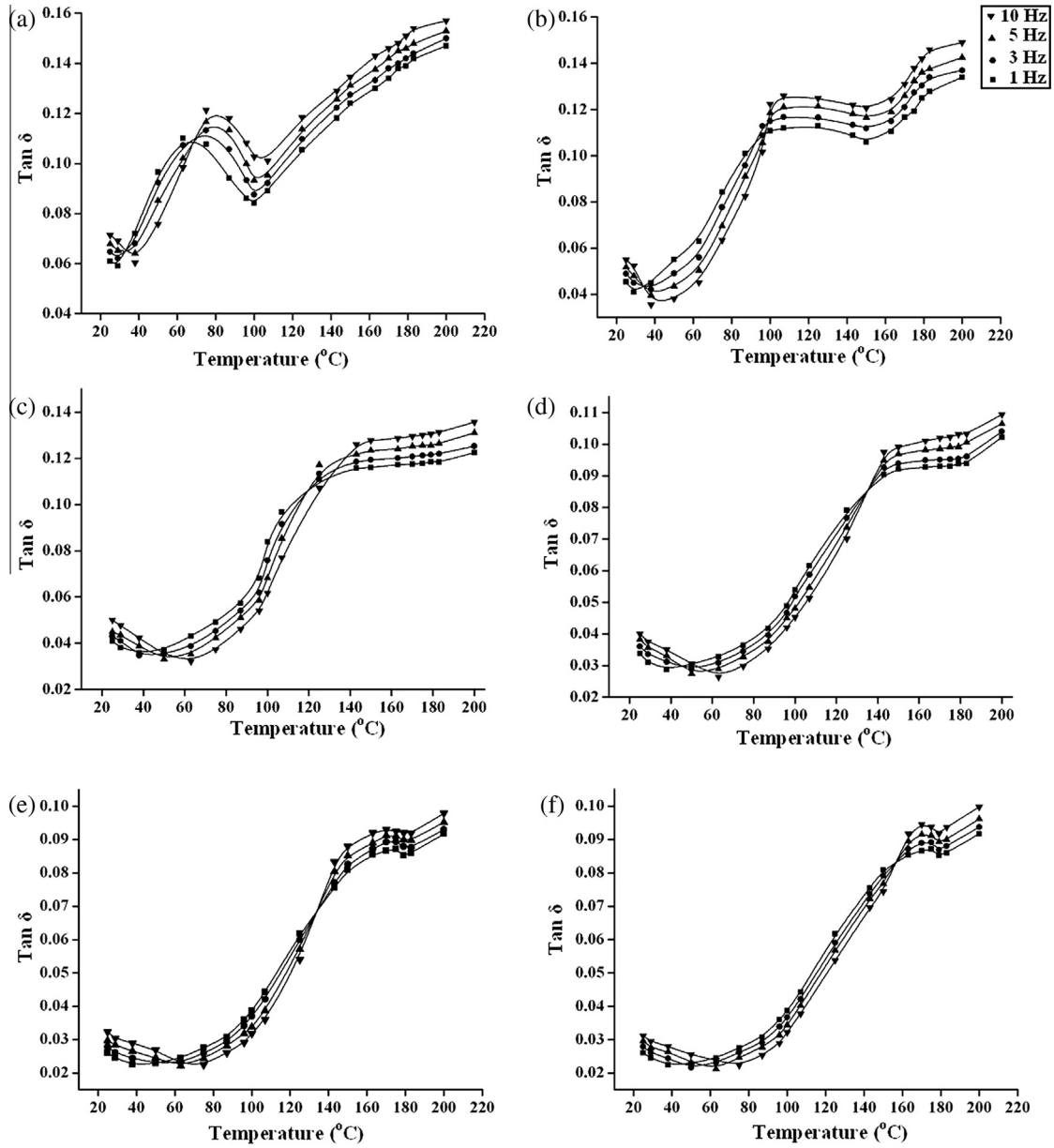

Fig. 8. Tan δ at different frequency range (a) untreated wood and wood treated with, (b) MFFA/DMDHEU, (c) MFFA/DMDHEU/nanoclay/MWCNT (0.5 phr), (d) MFFA/DMDHEU/nanoclay/MWCNT (1.0 phr), (e) MFFA/DMDHEU/MWCNT (1.5 phr) and (f) MFFA/DMDHEU/nanoclay/MWCNT (1.5 phr).

Table 2
Flexural and tensile properties of untreated and treated wood.

Sample	Flexural properties		Tensile properties	
	Strength (MPa)	Modulus (MPa)	Strength (MPa)	Modulus (MPa)
Untreated wood	120.3 (±2.2)	6047.4 (±3.1)	41.4 (±0.3)	307.7 (±11.3)
Wood treated with MFFA/DMDHEU	127.5 (±0.7)	6410.8 (±0.7)	52.3 (±0.5)	338.7 (±11.1)
MFFA/DMDHEU/MWCNT (1.5 phr)	154.8 (±0.7)	7764.3 (±0.6)	85.0 (±1.0)	631.7 (±9.3)
MFFA/DMDHEU/nanoclay/MWCNT (0.5 phr)	147.7 (±1.1)	7424.8 (±2.4)	78.6 (±1.0)	584.2 (±12.2)
MFFA/DMDHEU/nanoclay/MWCNT (1.0 phr)	152.4 (±1.0)	7661.4 (±4.1)	81.8 (±0.8)	607.9 (±10.1)
MFFA/DMDHEU/nanoclay/MWCNT (1.5 phr)	156.2 (±0.8)	7850.4 (±1.0)	86.3 (±1.1)	641.2 (±8.3)

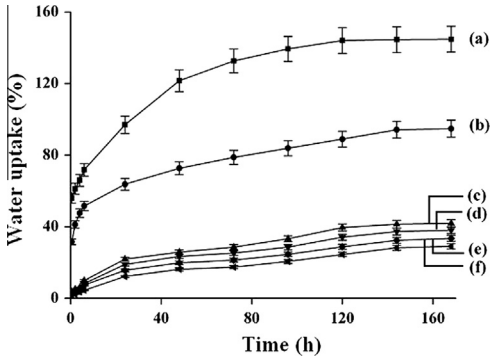

Fig. 9. Water uptake capacity of (a) untreated wood and wood treated with, (b) MFFA/DMDHEU, (c) MFFA/DMDHEU/nanoclay/MWCNT (0.5 phr), (d) MFFA/DMDHEU/nanoclay/MWCNT (1.0 phr), (e) MFFA/DMDHEU/MWCNT (1.5 phr) and (f) MFFA/DMDHEU/nanoclay/MWCNT (1.5 phr).

The higher interfacial adhesion between wood, polymer and crosslinker promoted better load transfer at the interface. Addition of MWCNT to the MFFA/DMDHEU enhanced the interaction through its surface hydroxyl groups which resulted in higher stress transfer at the interface. Samples treated with MFFA/DMDHEU/nanoclay/MWCNT exhibited an improvement in storage modulus of the composites as the silicate layers restricted the mobility of the polymer chains by fastening them into its gallery layers. At fixed loading of nanoclay, with the increase in the amount of MWCNT concentration, a further improvement in storage modulus value was observed.

4.6.2. Loss modulus

The loss moduli of untreated and treated wood samples are shown in Fig. 7B. All the loss modulus curves reached a maximum and then it decreased with the increase in the temperature because of the maximum dissipation of energy which occurred due to the free movement of the polymeric chains. MWCNT treated wood composites exhibited higher loss modulus than the untreated or the polymer treated wood composites. Nanoclay enhanced the interfacial interaction between wood and polymer resulting in improved E'' value. With the increase in the amount of MWCNT, an increase in the peak height for the loss modulus was observed. This occurred due to energy dissipation and inhibition of the relaxation process within the composite which contributed to an increase in internal friction.

4.6.3. Damping parameter ($\tan\delta$)

The variation of $\tan\delta$ as a function of temperature is shown in Fig. 7C. A reduction in peak height and broadening of the peak was observed for MFFA/DMDHEU treated samples in comparison with the untreated wood sample. A broader peak suggested a more time was needed for the relaxation of molecules due to lower polymeric chains movement resulting from formation of higher crosslinking density in the composites [30]. Further shifting of the peak to higher temperature was observed when MWCNT was added to the composite. MWCNT improved the interfacial adhesion that further reduced the peak intensity and shifted the peak to higher temperature [31]. The synergistic effect of nanoclay and MWCNT enhanced the interaction between wood and polymer through their surface hydroxyl groups leading to a more shifting of the peak. MWCNT in combination with nanoclay left a small part to deform at the interface and carried out a greater part of the force. Therefore, energy dissipation was less at the interface due to stronger interaction. The restriction in polymeric chain movement occurred in between the silicate layers. Higher the percentage of MWCNT, higher was the amount of shifting as well as decrease in peak height.

4.6.4. Effect of frequency

The viscoelastic properties of a material depend upon temperature and frequency. An increase in modulus values was obtained when frequency was varied as a function of temperature [32]. The variation of $\tan\delta$ values with frequency is represented in Fig. 8. An increase in peak height and shifting of glass transition temperature values were observed with the increase in frequency. The activation energy of the relaxation process for each composite can be calculated from the Arrhenius equation

$$\log f = \log f_o - E_a/2.303RT$$

where 'f', 'f_o', E_a, R and T denote the measured frequency, the frequency when the temperature approaches infinite, activation energy, universal gas constant and $\tan\delta$ maximum temperature respectively. Table 1 shows the activation energy for the relaxation process calculated from the slope of the plot of $\log f$ vs reciprocal of temperature. Higher value of activation energy was obtained for the treated wood samples. Nanoclay and MWCNT restricted the polymeric chain movement by increasing the interfacial interaction and stiffening the composites. Higher the amount of MWCNT, higher was the activation energy. Activation energy in the glass transition region was associated with the energy required for promotion of the initial movement of some molecular segments [33]. Higher activation required higher energy for initiation of polymer chain movement.

4.7. Tensile and flexural properties

Table 2 shows the tensile and flexural values of untreated and treated wood samples. Wood samples treated with MFFA/DMDHEU showed higher tensile and flexural values than the untreated wood samples. MF resin is one of the toughest polymeric resins that can enhance mechanical properties significantly and further DMDHEU could form a crosslinked structure with wood cell wall and polymer through its hydroxyl groups [18]. The incorporation of CNT enhanced the strength properties, MOE and modulus of rupture (MOR) of the composites. The surface hydroxyl groups present in modified MWCNT interacted with hydroxyl and methylol groups of wood, crosslinker and prepolymer resulting in enhanced properties. The MOE, MOR values improved further as

nanoclay was added to the samples treated with MFFA/DMDHEU/MWCNT. The nanoclay layers restricted the mobility of the polymer chains as they were fastened in between its gallery layers and hence stiffened the composites. At a fixed clay loading, the values enhanced remarkably with the increase in the amount of MWCNT.

4.8. Water uptake test

The water uptake test of untreated and treated wood samples is represented in Fig. 9. Untreated wood showed highest water absorption capacity as shown in curve a. The hydrophilic nature of wood was responsible for its highest water absorption capacity. Impregnation of wood with MFFA/DMDHEU would fill up its void spaces thereby decreasing its water uptake capacity. The hydroxyl groups present in DMDHEU could react with the methylol as well as hydroxyl groups of MFFA and the hydroxyl groups of wood cell wall forming a networked structure [18]. Samples treated with MFFA/DMDHEU/nanoparticles showed improved repellence to water. With the increase in the amount of MWCNT there was a further decrease in water absorption capacity. The surface hydroxyl groups of MWCNT would interact with nanoclay, MFFA, DMDHEU and wood with their hydroxyl groups and facilitates their deposition into the empty cell wall of wood and would make it more bulky.

5. Conclusion

The formation of MFFA and DMDHEU was confirmed from NMR study. XRD study demonstrated a decrease in crystallinity of wood cellulose as nanoclay and MWCNT was impregnated along with MFFA/DMDHEU into the composites. Raman spectroscopic analysis indicated surface modification of MWCNT and the formation of the composites. With the increase in the MWCNT content, the shifting of Raman 'G′-band occurred. This indicated an efficient load transfer as well as a good interfacial interaction between wood, polymer, nanoclay and MWCNT in the composite. SEM analysis revealed uniform distribution of nanoparticles in the composites. An improvement in elastic modulus, loss modulus and damping index was observed in WPC as indicated by DMA test. Tensile and flexural properties enhanced considerably for the wood samples treated with 3 phr nanoclay and 1.5 phr MWCNT. The water uptake capacity also decreased for the treated wood samples.

Appendix A. Supplementary material

Supplementary data associated with this article can be found, in the online version, at http://dx.doi.org/10.1016/j.cej.2014.02.069.

References

[1] S. Trey, S. Jafarzadeh, M. Johansson, In situ polymerization of polyaniline in wood veneers, ACS Appl. Mater. Interf. 4 (2012) 1760–1769.
[2] U.C. Yildiz, S. Yildiz, E.D. Gezer, Mechanical properties and decay resistance of wood–polymer composites prepared from fast growing species in Turkey, Bioresour. Technol. 96 (2005) 1003–1011.
[3] M.H. Schneider, A.E. Witt, History of wood polymer composite commercialization, Forest Prod. J. 54 (2004) 19–24.
[4] M.S. Islam, S.S. Hamdan, Z.A. Talib, A.S. Ahmed, M.R. Rahman, Tropical wood polymer nanocomposite (WPNC): the impact of nanoclay on dynamic mechanical thermal properties, Compos. Sci. Technol. 72 (2012) 1995–2001.
[5] Y. Gao, L.Y. Li, M. Mu, S. Osswald, Y. Gogotsi, K.I. Winey, An in situ Raman spectroscopy study of stress transfer between carbon nanotubes and polymer, Nanotechnology 20 (2009) 335703–335711.
[6] A. Thess, R. Lee, P. Nikolaev, H. Dai, Crystalline ropes of metallic carbon nanotubes, Science 273 (1996) 483–487.
[7] J.L. Bahr, J. Yang, D.V. Kosynkin, Functionalization of carbon nanotubes by electrochemical reduction of aryl diazonium salts: a bucky paper electrode, J. Am. Chem. Soc. 123 (2001) 6536–6542.
[8] N.A. Isitman, C. Kaynak, Polym. Degrad. Stab. 95 (2010) 1523–1532.
[9] B. Esteves, L. Nunes, H. Pereira, Properties of furfurylated wood (*Pinus pinaster*), Eur. J. Wood Prod. 69 (2011) 521–525.
[10] W. Gindl, F. Zargar-Yaghubi, R. Wimmer, Impregnation of softwood cell walls with melamine-formaldehyde resin, Bioresour. Technol. 87 (2003) 325–330.
[11] J.P. Lu, Elastic properties of carbon nanotubes and nanoropes, Phys. Rev. Lett. 79 (1997) 1297–1300.
[12] M. Corrias, P.H. Serp, P.H. Kalck, G. Dechambre, J.L. Lacout, C. Castiglioni, Y. Kihn, High purity multiwalled carbon nanotubes under high pressure and high temperature, Carbon 41 (2003) 2361–2367.
[13] B. Yi, R. Rajagopalan, H.C. Foley, U.J. Kim, X. Liu, P.C. Eklund, Catalytic polymerization and facile grafting of poly(furfuryl alcohol) to single-wall carbon nanotube: preparation of nanocomposite carbon, J. Am. Chem. Soc. 128 (2006) 11307–11313.
[14] D. Roy, S. Bhattacharyya, A. Rachamim, A. Plati, M.L. Saboungi, Measurement of interfacial shear strength in single wall carbon nanotubes reinforced composite using Raman spectroscopy, J. Appl. Phys. 107 (2010) 043501–043506.
[15] A. Hazarika, T.K. Maji, Synergistic effect of nano-TiO_2 and nanoclay on the ultraviolet degradation and physical properties of wood polymer nanocomposites, Ind. Eng. Chem. Res. 52 (2013) 13536–13546.
[16] A. Hazarika, T.K. Maji, Effect of different crosslinkers on properties of melamine formaldehyde-furfuryl alcohol copolymer/montmorillonite impregnated softwood (*Ficus hispida*), Polym. Eng. Sci. 53 (2013) 1394–1407.
[17] A.S. Angelatos, M.I. Burgar, N. Dunlop, F. Separovic, NMR structural elucidation of amino resins, J. Appl. Polym. Sci. 91 (2004) 3504–3512.
[18] Y. Xie, Z. Xiao, T. Grüneberg, H. Militz, C.A.S. Hill, L. Steuernagel, C. Mai, Effects of chemical modification of wood particles with glutaraldehyde and 1,3-dimethylol-4,5-dihydroxyethyleneurea on properties of the resulting polypropylene composites, Compos. Sci. Technol. 70 (2010) 2003–2011.
[19] S.M. Uddin, T. Mahmud, C. Wolf, C. Glanz, I. Kolaric, C. Volkmer, C.H. Holler, U. Wienecke, S. Roth, H.J. Fecht, Effect of size and shape of metal particles to improve hardness and electrical properties of carbon nanotube reinforced copper and copper alloy composites, Compos. Sci. Technol. 70 (2010) 2253–2257.
[20] A.Y. Cao, C.L. Xu, J. Liang, D.H. Wu, B.Q. Wei, X-ray diffraction characterization on the alignment degree of carbon nanotubes, Chem. Phys. Lett. 344 (2001) 13–17.
[21] J. Zhu, H. He, J. Guo, D. Yang, X. Xie, Arrangement models of alkylammonium cations in the interlayer of HDTMA+ pillared montmorillonites, Chin. Sci. Bull. 48 (2003) 368–372.
[22] W.H. Lü, G.J. Zhao, Z.H. Xue, Preparation and characterization of wood/montmorillonite nanocomposites, For. Stud. China 8 (2006) 35–40.
[23] A. Hazarika, T.K. Maji, Thermal decomposition kinetics, flammability, and mechanical property study of wood polymer nanocomposite, J. Therm. Anal. Calorim. http://dx.doi.org/10.1007/s10973-013-3394-7.
[24] R.R. Devi, T.K. Maji, Preparation and characterization of wood/styrene-acrylonitrile copolymer/MMT nanocomposite, J. Appl. Polym. Sci. 122 (2011) 2099–2109.
[25] A.M. Shanmugharaj, J.H. Bae, K.Y. Lee, W.H. Noh, S.H. Lee, S.H. Ryu, Physical and chemical characteristics of multiwalled carbon nanotubes functionalized with aminosilane and its influence on the properties of natural rubber composites, Compos. Sci. Technol. 67 (2007) 1813–1822.
[26] P. Tan, S.L. Zhang, K.T. Yue, F.J. Huang, Comparative Raman study of carbon nanotubes prepared by D.C. arc discharge and catalytic methods, Raman Spectr. 28 (1997) 369–372.
[27] N.G. Sahoo, Y.C. Jung, H.J. Yoo, J.W. Cho, Effect of functionalized carbon nanotubes on molecular interaction and properties of polyurethane composites, Macromol. Chem. Phys. 207 (2006) 1773–1780.
[28] L.S. Schadler, S.C. Giannaris, P.M. Ajayan, Load transfer in carbon nanotube epoxy composites, Appl. Phys. Lett. 73 (1998) 3842–3844.
[29] L. Liu, P.C. Maa, M. Xu, S. Ullah, J.K. Kim, Strain-sensitive Raman spectroscopy and electrical resistance of carbon nanotube-coated glass fibre sensors, Compos. Sci. Technol. 72 (2012) 1548–1555.
[30] A. Saiter, J.M. Saiter, C. Grenet, Cooperative rearranging regions in polymeric materials: relationship with the fragility of glass-forming liquids, Eur. Polym. J. 42 (2006) 213–219.
[31] A. Hernandez-Perez, F. Aviles, A. May-Pat, A. Valadez-Gonzalez, P.J. Herrera-Franco, P. Bartolo-Pérez, Effective properties of multiwalled carbon nanotube/epoxy composites using two different tubes, Compos. Sci. Technol. 68 (2008) 1422–1431.
[32] G. Roudaut, F. Poirier, D. Simatos, M.L. Meste, Can dynamical mechanical measurements predict brittle fracture behaviour?, Rheol Acta 44 (2004) 104–111.
[33] H.L. Ornaghi, A.S. Bolner, R. Fiorio, A.J. Zattera, S.C. Amico, Mechanical and dynamic mechanical analysis of hybrid composites molded by resin transfer molding, J. Appl. Polym. Sci. 118 (2010) 887–896.